

# Imperceptible Calibration for Radiometric Compensation

S. Zollmann and O. Bimber

Bauhaus-University Weimar, Germany

---

## Abstract

We present a novel multi-step technique for imperceptible geometry and radiometry calibration of projector-camera systems. Our approach can be used to display geometry and color corrected images on non-optimized surfaces at interactive rates while simultaneously performing a series of invisible structured light projections during runtime. It supports disjoint projector-camera configurations, fast and progressive improvements, as well as real-time correction rates of arbitrary graphical content. The calibration is automatically triggered when misregistrations between camera, projector and surface are detected.

Categories and Subject Descriptors (according to ACM CCS): H.5.1 [INFORMATION INTERFACES AND PRESENTATION]: Multimedia Information Systems Artificial, Augmented, and Virtual realities; I.3.3 [Computer Graphics]: Picture/Image Generation I.4.8 [Image Processing and Computer Vision]: Scene Analysis

---

## 1. Introduction and Motivation

Projections onto complex everyday surfaces is challenging. Projector-camera systems together with appropriate scene analysis techniques and real-time image correction methods can improve the quality of graphical content projected on such surfaces. To support this, surface properties, such as geometry and reflectance parameters, need to be scanned in advance before using them for image corrections during run-time. This is known as *radiometric compensation* [NPGB03], [BEK05], [FGN05]. In most cases, a one-time calibration process applies visible structured light projection and camera feedback to establish the correspondence between camera and projector pixels and to measure the radiometric behavior of the surface pigments. The mappings and color values can be stored in look-up textures that can be processed by the GPU to perform pixel-displacement mapping and a pixel-precise color compensation in real-time [BEK05]. For many applications, however, a frequent re-calibration is necessary because the alignment of camera and projectors with the surfaces changes over time (e.g., due to mechanical expansion through heating, accidental offset, intended readjustment). In these cases, it is not desired to disrupt a presentation with visible light patterns.

## 2. Related and Previous Work

A first proof of concept for embedding invisible structured light patterns into DLP projections was introduced in [RWC\*98]. In this work, binary codes have been embedded by projecting temporally alternating code images and their complements. A variation of this approach was applied by [WWC\*05] and [VVSC05] for 3-D video acquisition. In all cases, however, the projected patterns are well detectable by human observers. Even in [RWC\*98] the code patterns must be visible during eye movements<sup>†</sup> and while temporal code transitions. In [GSHB07] properties of human perception are taken into account for adapting the coding parameters depending on local characteristics of image and code. This makes a truly imperceptible temporal coding of binary information possible. Cotting et. al. introduced a coding scheme [CNGF04] that synchronizes a camera to a specific time slot of a DLP micro-mirror flipping sequence in which imperceptible binary patterns are embedded. However, not all mirror states are available for all possible intensities. To still achieve the desired binary value during this period, color values of the original image have to be adjusted. This results in a tonal shift of the original image, which can be high - especially for upper and lower intensity ranges. Dynamic

---

<sup>†</sup> caused by visual perception effect called *phantom-array*

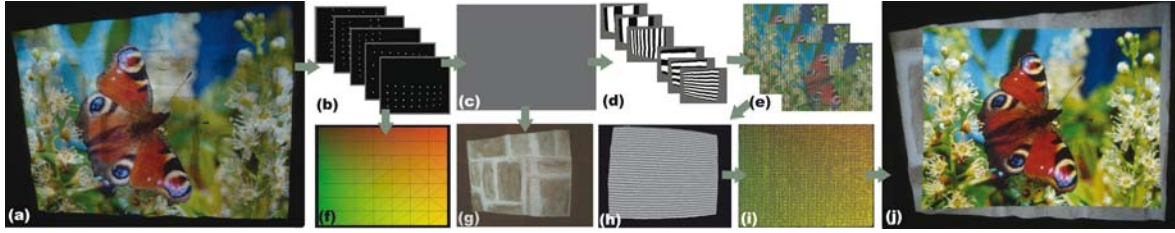


**Figure 1:** A series of invisible patterns (b-e) integrated into an image (a) and projected onto a complex surface (g) results in surface measurements (f-i) used for radiometric compensation (j).

range reductions of up to 40-50% have been reported, and only geometric calibrations are achieved.

Instead of visible or invisible structured light projections, features of the captured distorted projection can be analyzed to support the calibration of a projector-camera systems. A first example was presented in [YW01], while advanced variations have been described later. The possibility of establishing the correspondence between projector and camera pixels in these cases, however, depends on the quality of the detected images features. Consequently, this is not independent on the projected content. Again, only geometric corrections and simple intensity adjustments are currently supported by such techniques.

Fujii et al. have described a dynamically adapted radiometric compensation technique that supports changing projection surfaces and moving projector-camera configurations [FGN05]. Their system requires a fixed co-axial alignment of projector and camera. An optical registration of both devices makes a geometric calibration unnecessary. Since a strict optical alignment is not possible in every case, such an approach is too inflexible for many applications (e.g., when multiple projectors are mounted at locations that are different from the position of the calibration camera). Furthermore, the quality of the radiometric compensation strongly depends on the projected image content.

Our technique applies a temporal coding that is based on [RWC\*98] with enhancements for human visual perception [GSHB07]. Projectors and camera do not have to be mechanically or optically aligned. Geometric registration as well as radiometric measurements are achieved through a well-cosen series of invisible structured light patterns embedded into the projected content (cf. figure 1). Images are projected at interactive frame rates, while the image quality is progressively improved after geometric mis-alignments are detected automatically.

### 3. Coding and Reconstruction

For embedding a binary pattern  $C$  into the projected original image  $O$ , a code image  $P_{code}$  can be calculated by adding a small value  $\Delta$  onto  $O$  to encode a binary 1, or subtracting  $\Delta$

from  $O$  for encoding a binary 0. Thereby,  $O$  might have to be scaled to  $\Delta \leq O \leq 1 - \Delta$ . However, since  $\Delta$  is small (3-5% of the total intensity range in our case), this does not influence the visual appearance of  $O$  much. When displaying, the projected code image must be compensated by its complementary image  $P_{comp} = O - P_{code}$ . Projecting these two images with a refresh rate above the critical flicker frequency, one perceives the temporal integration of both (approx.  $(P_{code} + P_{comp})/2$ ). A dynamic adaptation of  $\Delta$  based on local image properties, such as spatial frequencies and local luminance in  $O$  and  $C$  will ensure that the code remains invisible even through fast eye-movements and temporal code transitions, as explained in [GSHB07]. A synchronized calibration camera that captures both images ( $P_{code}$  and  $P_{comp}$ ) can reconstruct the code ( $C = ((P_{code} - P_{comp}) <=> 0)$ ). This method is robust against noise and invariant of the surface reflectance. As explained in section 4 it is used in early calibration steps that apply fast binary code patterns, such as points or stripes (cf. figures 1b,d).

To encode intensity values ( $C = \Delta$ ) instead of binary values,  $O$  is multiplied by  $\Delta$  to compute the code image ( $P_{code} = O\Delta$ ). The compensation image is then given by  $P_{comp} = O(2 - \Delta)$ , and the embedded code can be reconstructed from both images with  $C = \Delta = 2P_{code}/(P_{code} + P_{comp})$ . Embedding intensities offers the possibility to use advanced geometric calibration techniques, such as phase shifting [HZ06]. It is used by later calibration steps (cf. figure 1e) that deliver precise geometric mappings (explained in section 4). Instead of a local adaptation of  $\Delta$  as for binary coding, only a global adjustment based on average properties (spatial frequency and luminance) of  $O$  and  $C$  can be used for intensity coding to preserve the correct intensity values.

Instead of embedding binary or intensity values into the gray channel, all three color channels can be encoded differently. This, however, requires neutralizing the mixing among different color channels caused by projector filters and camera sensor. Determining and applying color transformation is a common technique for radiometric compensation (e.g., [NPG03], [FGN05]), which has to be applied in this case as well. Yet, we found that color coding is quite unreliable for almost all embedded intensity codes and even for most binary codes that are projected on textured and colored sur-

faces. Thus we use the gray channel only for the sake of stability. Note, that a correct coding and decoding is only possible if projectors and camera are linearized. A gamma correction on  $O$  is required before embedding the code. This satisfies the non-linear response of the human visual system. All coding, decoding and correction calculations are carried out with fragment shaders on the GPU to achieve real-time performance on a per-pixel basis.

#### 4. Multi-Step Calibration

Based on the coding techniques described in section 3, we propose a multi-step calibration process that aims at delivering approximated results quickly, while carrying out subsequent progressive improvements. All steps are imperceptible while presenting graphical or video content at interactive frame rates.

A constant dense pattern of binary points is encoded and projected continuously. A mis-registration between projector, camera and surface is detected automatically if the binary difference between two subsequent captured code patterns is above a predefined threshold. The re-calibration is triggered immediately after subsequent code patterns match again (following an earlier mis-registration). The three calibration steps and their produced results are illustrated in figure 1.

*Step 1:* A sequence of binary point codes (cf. figure 1b) is projected to sample pixel correspondences between projector and camera. Since only discrete positions are measured but a continuous look-up table is required for pixel-displacement mapping on the GPU, intermediate values have to be interpolated. This is achieved by a Delaunay triangulation and an interpolation of the 2D displacement samples during off-screen rendering. The resulting look-up texture (cf. figure 1f) is passed to the GPU for geometric image correction [BEK05]. A coarse geometric registration is the result of step 1 (cf. figure 2c).

*Step 2:* The surface reflectance is analyzed next by embedding a uniform gray image  $I$  into the projection (cf. figure 1c). Capturing the surface under a uniform gray illumination results in a diffuse reflectance map (cf. figure 1g) that is required by compensation techniques, such as [BEK05]. The advantage of this is, that in contrast to the method used in [FGN05], this approach is independent of the image content, and therefore more reliable. However, the original image  $O$  has to provide a global minimum gray level of  $I$ . If this is not the case,  $O$  is increased slightly in brightness. Note that this does not result in local tonal shifts, as in [CNGF04]. Depending on the exposure times and projector brightness,  $I$  can be fairly small (3-5% of the total intensity range in our case). Thus, while  $P_{code} = I$  and  $P_{comp} = O - P_{code}$ , the perceived result is  $(P_{code} + P_{comp})/2$ , and the embedded gray image is not visible.

*Step 3:* The system is now roughly calibrated and displays

an approximated result. If no further mis-registrations are detected, a more accurate (but also more time-consuming) calibration step is triggered. It is based on the 3-step phase shifting algorithm described in [HZ06], which measures precise correspondences for each projector/camera pixel. For phase shifting, three sinusoidal patterns (each shifted by 120 degree,  $-120^\circ$  for  $I_1$ ,  $0^\circ$  for  $I_2$  and  $+120^\circ$  for  $I_3$ ) have to be projected for  $x$  and  $y$  directions (cf. figure 1e for  $x$ ). The captured images are used to convert the decoded intensities into wrapped phase values for each pixel (cf. figure 1h for  $y$ ), as in [HZ06]:

$$\phi_{rel}(x,y) = \arctan\left(\sqrt{3} \frac{I_1 - I_3}{2I_2 - I_1 - I_3}\right) \quad (1)$$

The results of equation 1 ranges from  $-\pi$  to  $\pi$  and are called *wrapped phase values*. In this context “wrapped” refers to the fact that the phase values contain discontinuities. For deriving continuous phase values (called *unwrapped* or *absolute phase map*) a transformation from relative values to absolute values has to be applied. This transformation depends on the characteristic of the underlying surface. For geometries consisting of one single-connected component the phase unwrapping technique described in [ZLY07] can be used. It removes the  $2\pi$  discontinuities from wrapped phase values by examining the phase map gradients using two additional maps indicating the quality of the calculated phase values. For geometries consisting of non-connected components the projected calibration image is divided in to several rectangular regions first, whereas each region is defined by the periods of the relative phase values. The region map, that is applied to transform the phase values into absolute values, is determined by projecting  $2ld(r)$  additional gray code patterns (cf. figure 1d), where  $r$  is the number of different regions. The unique gray code  $k$  of each region is multiplied with  $2\pi$  and added to the relative phase values. This results in absolute phase values ( $\phi_{abs} = k2\pi + \phi_{rel}$ ).

After transforming the relative phase values into absolute ones, triangulation and interpolation creates a continuous look-up table (cf. figure 1i). This allows for a pixel-precise update of the previous geometric calibration (cf. figure 2d). An additional reflectance analysis is not necessary. All computations are carried out in fragment shaders on the GPU.

#### 5. Summary and Future Work

In this paper we presented a multi-step, imperceptible calibration technique for projector-camera systems. To our knowledge, this is the first imperceptible calibration approach that 1) enables radiometric measurements independent of the image content, 2) supports intensity coding, and 3) allows a pixel-precise geometric calibration that neither requires a fixed optical alignment nor a static (pre-calibrated) projector-camera arrangement. Our system applies a series of invisible structured light patterns to detect mis-registrations, to compute and display corrected image quickly, and to improve the results progressively. The visual

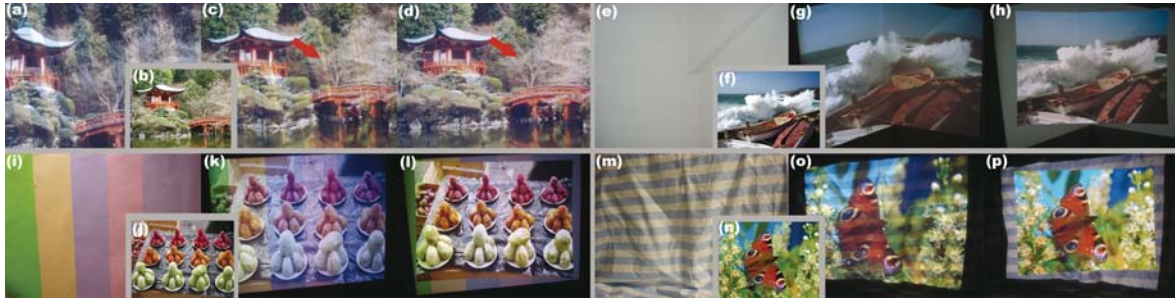


**Figure 2:** Sample results for different surfaces and multiple images: originals (b,f,j,n), without compensation (a,g,k,o) and with compensation (c,d,h,l,p). Close-up after step 2 with slight error (c) and close-up after step 3 (d).

quality of the displayed images, such as tonal shifts or extreme dynamic range reductions, is -except to a small constant scaling in brightness- not influenced.

Assuming that  $b$  blending steps are required for seamless code transitions, as explained in [GSHB07],  $ld(p)b_1$  code images have to be captured for steps 1, where  $p$  is the number coded binary points. For step 2,  $b_2$  code images have to be captured. The optional gray code projection in step 3 requires to capture  $2ld(r)b_3$  code images (for  $x$  and  $y$  directions), while for the intensity-based phase-shifting  $6b_4$  code images are necessary (for  $x$  and  $y$  directions). Currently, at least  $50ms$  are required for acquire one code pattern (by capturing  $P_{code}$  and  $P_{comp}$ ), image processing, coding/decoding computations and content rendering. This is equivalent to a frame rate of  $20Hz$  for content presentation with simultaneous calibration. However, the sub-images  $P_{code}$  and  $P_{comp}$  are continuously projected with a constant speed of  $120Hz$ , resulting in a perceived refresh rate of  $60Hz$ . If for instance, as in our applications,  $b_1 = 4$ ,  $b_2 = 10$ ,  $b_3 = b_4 = 8$ ,  $p = 64$  and  $r = 32$  is required, then an approximated re-calibration can be displayed after  $1.7s$ , while the high-quality update can be delivered after additional  $6.4s$ . A decrease of the overall calibration time can be achieved by multi-threading. Although the projection sequence remains sequential, demanding computations could be processed during projection and capturing. This optimization belongs to our future work. Furthermore, we want to investigate perception-based image adaptation techniques [GB07] that allow to dynamically increase the local brightness in  $O$  (for ensuring the minimum gray level required for the reflectance measurements) while minimizing the perceived difference to the unadapted version of  $O$ .

## References

- [BEK05] BIMBER O., EMMERLING A., KLEMMER T.: Embedded entertainment with smart projectors. *IEEE Computer* 38 (2005), 48–55.
- [CNGF04] COTTING D., NAEF M., GROSS M., FUCHS H.: Embedding imperceptible patterns into projected images for simultaneous acquisition and display. In *ISMAR '04: Proceedings of the Third IEEE and ACM International Symposium on Mixed and Augmented Reality (ISMAR '04)* (Washington, DC, USA, 2004), IEEE Computer Society, pp. 100–109.
- [FGN05] FUJII K., GROSSBERG M., NAYAR S.: A projector-camera system with real-time photometric adaptation for dynamic environments. pp. I: 814–821.
- [GB07] GRUNDHÖEFER A., BIMBER O.: Real-time adaptive radiometric compensation. *To appear in Transactions on Visualization and Graphics* (2007).
- [GSHB07] GRUNDHÖEFER A., SEEGER M., HÄNTSCH F., BIMBER O.: Coded projection and illumination for television studios. *Technical Report no. 843, Bauhaus-University Weimar* (2007).
- [HZ06] HUANG P. S., ZHANG S.: Fast three-step phase-shifting algorithm. *Appl. Opt.* 45, 21 (2006), 5086–5091.
- [NPG03] NAYAR S. K., PERI H., GROSSBERG M. D., BELHUMEUR P. N.: A projection system with radiometric compensation for screen imperfections. In *Proc. ICCV Workshop on Projector-Camera Systems (PRO-CAMS)* (2003).
- [RWC\*98] RASKAR R., WELCH G., CUTTS M., LAKE A., STESIN L., FUCHS H.: The office of the future: a unified approach to image-based modeling and spatially immersive displays. In *SIGGRAPH '98: Proceedings of the 25th annual conference on Computer graphics and interactive techniques* (New York, NY, USA, 1998), ACM Press, pp. 179–188.
- [VVSC05] VIEIRA M. B., VELHO L., SA A., CARVALHO P. C.: A camera-projector system for real-time 3d video. In *CVPR '05: Proceedings of the 2005 IEEE Computer Society Conference on Computer Vision and Pattern Recognition (CVPR '05) - Workshops* (Washington, DC, USA, 2005), IEEE Computer Society, p. 96.
- [WWC\*05] WASCHBÜSCH M., WÜRMLIN S., COTTING

- D., SADLO F., GROSS M. H.: Scalable 3d video of dynamic scenes. *The Visual Computer* 21, 8-10 (2005), 629–638.
- [YW01] YANG R., WELCH G.: Automatic and continuous projector display surface calibration using every-day imagery. In *WSCG 2001 Conference Proceedings* (2001), Skala V., (Ed.).
- [ZLY07] ZHANG S., LI X., YAU S.-T.: Multilevel quality-guided phase unwrapping algorithm for real-time three-dimensional shape reconstruction. *Applied Optics* 46, 1 (2007), 50–57.